*Work supported by the U. S. Atomic Energy Commission.

†Presently at Columbia University, New York, N. Y.
‡Presently at California State College at Sonoma, Rohnert Park, Calif.
§Presently at Lawrence Radiation Laboratory, Berkeley, Calif. 94720.
‖Presently at Cornell University, Ithaca, N. Y. 14850.

[1]M. Goitein, R. J. Budnitz, L. Carroll, J. R. Chen, J. R. Dunning, Jr., K. Hanson, D. C. Imrie, C. Mistretta, and Richard Wilson, Phys. Rev. D 1, 2449 (1970).
[2]W. T. Scott, Rev. Mod. Phys. 35, 231 (1963).
[3]G. F. Dell and M. Fotino, Cambridge Electron Accelerator Laboratory Report No. CEAL-1045, 1968 (unpublished).
[4]P. F. Cooper (private communication).
[5]H. Winick, Cambridge Electron Accelerator Laboratory Report No. CEAL-1015, 1964 (unpublished).
[6]L. W. Mo and Y. S. Tsai, Rev. Mod. Phys. 41, 205 (1969).
[7]Y. S. Tsai, Phys. Rev. 122, 1898 (1960).
[8]N. Meister and D. R. Yennie, Phys. Rev. 130, 1210 (1963).
[9]D. R. Yennie, S. C. Frautschi, and H. Suura, Ann. Phys. (N. Y.) 13, 379 (1961).
[10]D. H. Coward, H. De Staebler, R. A. Early, J. Litt, A. Minten, L. W. Mo, W. K. H. Panofsky, R. E. Taylor, M. Breidenbach, J. I. Friedman, H. W. Kendall, P. N. Kirk, B. C. Barish, J. Mar, and J. Pine, Phys. Rev. Letters 20, 292 (1968).
[11]Chr. Berger, E. Gersing, G. Knop, B. Langenbeck, K. Rith, and F. Schumacher, Phys. Letters 26B, 276 (1968); Chr. Berger, V. Burkert, G. Knop. B. Langenbeck, and K. Rith (unpublished).
[12]W. Bartel, B. Dudelzak, H. Krehbiel, J. M. McElroy, U. Meyer-Berkhout, R. J. Morrison, H. Nguyen Ngoc, W. Schmidt, and G. Weber, Phys. Rev. Letters 17, 608 (1966); Phys. Letters 25B, 236 (1967).
[13]T. Janssens, R. Hofstadter, E. B. Hughes, and M. R. Yearian, Phys. Rev. 142, 922 (1966).
[14]P. Lehmann, R. Taylor, and Richard Wilson, Phys. Rev. 126, 1163 (1962); B. Dudelzak, G. Sauvage, and P. Lehmann, Nuovo Cimento 28, 18 (1963).
[15]W. Albrecht, H. J. Behrend, F. W. Brasse, W. Flauger, H. Hultshig, and K. G. Steffen, Phys. Rev. Letters 17, 1192 (1966).
[16]W. Bartel, F.-N. Büsser, W.-R. Dix, R. Felst, D. Harms, H. Krehbiel, P. E. Kuglman, J. McElroy, and G. Weber, Phys. Letters 33B, 245 (1970).
[17]S. I. Bilenkaya, Yu. M. Kazarinov, and L. I. Lapidus, paper submitted to the Fifteenth International Conference on High Energy Physics, Kiev, USSR, 1970 (unpublished).
[18]J. Litt, G. Buschhorn, D. H. Coward, H. DeStaebler, L. W. Mo, R. E. Taylor, B. C. Barish, S. C. Loken, J. Pine, J. I. Friedman, G. C. Hartman, and H. W. Kendall, Phys. Letters 31B, 40 (1970).

PHYSICAL REVIEW D VOLUME 4, NUMBER 1 1 JULY 1971

Search for Ionizing Tachyon Pairs From 2.2-GeV/c K^-p Interactions*

Jerome S. Danburg, George R. Kalbfleisch, Samuel R. Borenstein,†
Richard C. Strand, and Vance VanderBurg
Physics Department, Brookhaven National Laboratory, Upton, New York 11973

and

J. W. Chapman and J. Lys
Department of Physics, University of Michigan, Ann Arbor, Michigan 48104
(Received 4 March 1971)

We have searched for pairs of charged particles t^+t^- with spacelike four-momenta produced in K^-p interactions at 2.2 GeV/c. It was assumed that such particles could produce visible tracks in the bubble chamber. Under the additional assumption that only tachyons with velocities not much greater than the speed of light ($v \lesssim 1.7c$) could produce visible tracks, the experiment would be sensitive to tachyon invariant masses $\mu = (-p \cdot p)^{1/2}$ between 100 MeV and 1 GeV and to tachyon-pair invariant-mass-squared values between 0 and 1.44 GeV^2. No example of the reaction $K^-p \to \Lambda t^+t^-$ was found (for momentum transfer squared between 0 and -0.8 GeV^2), implying a cross section upper limit of ≈ 0.2 μb.

I. INTRODUCTION

Since the discussion of the possibility of faster-than-light particles in the framework of the special theory of relativity was initiated by Bilaniuk, Deshpande, and Sudarshan[1] in 1962, this topic has attracted considerable theoretical interest. Such particles would obey the relations

$$E = \frac{\mu}{(v^2-1)^{1/2}}, \quad |\vec{p}| = \frac{\mu v}{(v^2-1)^{1/2}}$$

and thus

$$E^2 - \vec{p}^2 = -\mu^2 < 0, \quad v = |\vec{p}|/E > 1.$$

(We use the convention $c \equiv 1$ in this paper.)

Feinberg[2] has formulated a quantum field theory of faster-than-light particles, for which he has introduced the name "tachyons." Arons and Sudarshan[3] and Dhar and Sudarshan[4] have continued the discussion of the quantum field theory of tachyons. Other theoretical aspects of the description of tachyons,[5-14] especially causality effects associated with the existence of tachyons,[15-23] have been discussed in the recent literature. Several of these theoretical problems, and some other topics related to tachyons, as propounded by a number of authors, are examined in two articles in *Physics Today*.[24]

Two accounts of experimental searches for tachyons have been published.

Using the fact that it is kinematically possible for a system with any value of invariant mass squared to decay into a pair of tachyons, each having invariant mass μ, for any value of μ, Alväger and Kreisler[25] have tried to detect tachyons presumed to be produced by γ rays of several hundred keV incident on lead. These authors have shown that if tachyons thus produced emitted Čerenkov radiation analogous to that of ordinary particles, then the tachyons, when traveling along the lines of an electric field in the experimental apparatus, could be imparted energy which would be radiated away as Čerenkov light and detected in a photomultiplier. This search produced a null result. In order to facilitate a comparison of this search with the search performed in the present experiment, we list the major assumptions involved in the experiment of Alväger and Kreisler. Besides the assumptions that tachyons indeed exist and that charged tachyons can be produced by γ rays with energies somewhat less than 1 MeV, in this search it was assumed (1) that charged tachyons emit Čerenkov radiation in vacuum which can be calculated analogously to that of ordinary charged particles in matter; (2) that charged tachyons gain energy in an electric field just as ordinary charged particles do; (3) that tachyons are not very likely to be captured in matter; (4) that the tachyons have charge between about $0.1e$ and $2e$.

Baltay, Feinberg, Yeh, and Linsker[26] have performed a search for neutral (or at least unseen) tachyons produced singly or in pairs by the interactions of stopped K^- and $\bar{p}$ with protons in a bubble chamber. This search was independent of the interactions of the tachyons assumed to be produced; it made use of the facts that the invariant mass squared of a single tachyon is always negative, and that a pair of tachyons may have negative as well as positive invariant mass squared. There was no evidence for negative mass-squared systems recoiling against normal final-state particles for either incident K^- or $\bar{p}$. The search for singly produced neutral tachyons in these bubble-chamber exposures involves no assumptions beyond the defining energy-momentum relationship of tachyons. The search for pairs of neutral tachyons required, in addition to the above, only the assumption that the matrix element for neutral tachyon pair production does not strongly suppress the production of pairs with negative mass squared, even though a considerable fraction of phase space gives negative mass squared for tachyon pairs.

In Sec. II we discuss the method applied in the present experiment to search for charged tachyon pair production. Section III contains a discussion of the phase space and the final-state Dalitz plot for the reaction $K^-p \to \Lambda +$ tachyon pair. The analysis of the bubble-chamber pictures and the results of the search are given in Sec. IV, and our conclusions are stated in Sec. V.

II. EXPERIMENTAL METHOD

In the present experiment we examine reactions of the form

$$K^-p \to \Lambda + \text{two charged tracks}, \quad \Lambda \to p\pi^- \tag{2.1}$$

for 2.2 GeV/c K^- from the Brookhaven AGS incident on the 31-in. BNL bubble chamber filled with a hydrogen-neon mixture. The quantity of film (400 000 pictures) examined for this search corresponds to a beam path length of ≈ 20 events/μb. We wish to investigate whether any of the pairs of charged particle tracks produced with a Λ can be determined to be those of tachyons; that is, we look for the reaction

$$K^-p \to \Lambda t^+ t^-, \tag{2.2}$$

where $t^{\pm}$ denotes a charged tachyon.

The fact that we seek charged-tachyon tracks in the bubble chamber directly implies the following assumptions:

(1) Tachyons are charged and tachyons of a given momentum follow curved paths in a magnetic field just as singly charged ordinary particles of the same momentum do.

(2) Tachyons leave ionized tracks in the bubble chamber with bubble densities comparable to that of ordinary charged particles. This assumption will be restricted to hold only for tachyons with velocities close to that of light, i.e., for $v \lesssim 1.7c$. This restriction will in turn yield an effective upper limit for the tachyon invariant mass μ, as is discussed below.

(3) The Čerenkov radiation of charged tachyons is suppressed sufficiently to allow ionization to be

the dominant energy-loss mechanism.

We will return to a discussion of these assumptions and compare them with those of the other two published tachyon searches after presenting the method used here.

In the usual analysis of reaction (2.1) occurring in a bubble chamber, assuming that a Λ decay has been positively identified, the two charged tracks are taken to be kaons or pions. Assume for the moment that the charged tracks were made by tachyons and that there are no invisible neutral particles in the final state; i.e., assume reaction (2.2). Then the interpretation of the charged tracks as those of pions or kaons would result in the assignment of too much energy to the outgoing charged particles, since a tachyon's momentum is always greater than its energy, while the reverse is true for ordinary particles. The least amount of energy is assigned to the final-state particles when the outgoing tracks are interpreted as pions (we do not fit outgoing primary interaction tracks as muons or electrons), and in this case there is of course still too much energy assigned to the final state. For each example of reaction (2.1) the outgoing charged tracks from the primary interaction vertex are interpreted as pions, and the missing energy and momentum necessary for energy and momentum balance are calculated using the measured momentum for the visible charged tracks; that is, each event is interpreted as

$$K^-p \to \Lambda\pi^+\pi^-(\mathrm{MM}). \tag{2.3}$$

If the tracks which are interpreted as pions are really tachyons, the momentum of the neutral system denoted by (MM) will be close to zero (within the error given by the measurement of the visible tracks), assuming, as we have done, that the momentum of the tachyons is correctly measured. The energy of the assumed neutral particle(s) will be negative and thus the invariant mass squared of the (MM) system will be positive, within errors. The method used to detect whether some events of the type (2.1) are examples of charged tachyon pair production via reaction (2.2) consists of an examination of all events for which the calculated missing energy is negative when the event is interpreted as reaction (2.3). Particular attention is devoted to those events which cannot be successfully fitted to a reaction hypothesis in which the neutral system denoted by (MM) is a single ordinary particle (γ, π^0, or η) or no particle at all.

Now that the method of detecting tachyon pairs has been outlined, we return to an evaluation of the assumptions we have made about the properties of tachyons. The expected electromagnetic properties of tachyons given in assumptions (1) and (2) are those of ordinary particles. In the second assumption we mean that the bubble density of charged tachyons should vary as $1/\beta^2$; the above-mentioned restriction to $\beta \lesssim 1.7$ thus ensures that we study tracks not more than about a factor of 3 lighter than "maximum-ionizing" tracks. Having assumed that tachyons may be electromagnetically similar to ordinary particles in two respects, it may seem unappealing to assume an important difference in a third respect, that of Čerenkov-radiation emission. Reference 25 contains a calculation of tachyon Čerenkov-radiation energy loss per unit path length, assuming that tachyons emit Čerenkov radiation just as ordinary particles do. There it is shown that if a tachyon is produced with an energy comparable to μc^2 ($-\mu^2$ = invariant mass squared of the tachyon), the tachyon will travel only ≈ 50 μ before Čerenkov radiation reduces its energy to 1 eV. Therefore the assumption that Čerenkov radiation is somehow suppressed in order to allow the tachyons to retain large energies over considerable track lengths is a departure from the properties of ordinary particles. Nevertheless, it is felt that the lack of *a priori* knowledge of the properties of tachyons, and the unambiguous kinematical characteristics of reaction (2.2) if visible ionization tracks are produced, justify a search for tachyon pair production in the manner described above.

The search for neutral tachyon pair production in $\bar{p}p$ and K^-p interactions described in Ref. 26 was confined to negative mass squared for the tachyon pairs. For the reactions studied in this reference, tachyon pairs with negative invariant mass squared occur for a considerable fraction of the phase space. If, however, the matrix element for tachyon pair production were not constant over the phase space, but if, for instance, tachyon pairs were produced primarily or entirely through the decay of meson resonances, then tachyon pairs with negative invariant mass squared might be considerably less likely than those with positive mass squared. This possible preference for positive mass-squared pairs would of course depend on the mass and width of the meson resonances which might decay into tachyon pairs, as well as on the amount of nonresonant pair production. The present experiment is primarily sensitive to tachyon pairs with positive invariant mass squared, as will be discussed below. Thus if tachyon pairs with positive invariant mass squared are more likely than those with negative mass squared, the present search for charged tachyon pairs would be more sensitive than the search of Baltay, Feinberg, Yeh, and Linsker[26] for neutral pairs. Of course, the present search entails more assumptions about the properties of tachyons than that of Ref. 26.

III. PHASE SPACE FOR $K^-p \to \Lambda t^+ t^-$

It is interesting that the phase space for this reaction is different in different Lorentz frames. This comes about because there are Lorentz transformations which convert a positive-energy tachyon in one frame into a negative-energy tachyon in another. In order to avoid negative-energy particles, it is possible to reinterpret a negative-energy tachyon as a positive-energy tachyon traveling backward in time.[1,2] A possible final-state configuration in one Lorentz frame can give a negative-energy tachyon in a second frame; in the second frame this tachyon would be interpreted as an *incoming* particle. This means that a configuration corresponding to the reaction

$$K^- + p \to \Lambda + t^+ + t^- \tag{3.1}$$

in one Lorentz frame can correspond to the reaction

$$K^- + p + t^\pm \to \Lambda + t^\pm \tag{3.2}$$

or

$$K^- + p + t^+ + t^- \to \Lambda \tag{3.3}$$

in another frame. Thus if we insist on dealing only with reaction (3.1) and not with (3.2) or (3.3), there will be a different final-state Dalitz plot for reaction (3.1) in different frames. Reference 26 contains a calculation of the tachyon-pair phase space for reaction (3.1) in the c.m. frame (which is also the laboratory frame for the stopped K^- used in the search of this reference). Below we describe the c.m. Dalitz plot for reaction (3.1), from which the $\Lambda t^\pm$ phase space as well as the t^+t^- phase space can be deduced. The laboratory-frame Dalitz plot is also described, and the connection between the Dalitz plots in the two frames is discussed. The laboratory-frame t^+t^- phase space is also given below; it is needed to estimate tachyon-pair production rates.

In a number of the final-state configurations on the boundary of the Dalitz plots discussed below, for at least one of the tachyons $p = \mu = [-(\text{invariant mass squared})]^{1/2}$, $E = 0$, $v = \infty$. We propose calling this condition the "liberty" state of a tachyon. The terms "at rest" (when $p = 0$, $E = m$, $v = 0$), "rest mass," and "rest energy" applied to ordinary particles are replaced by the suggestive analogous terms "at liberty" (when $p = \mu$, $E = 0$, $v = \infty$), "liberty mass," and "liberty momentum," respectively, for tachyons. We will use this nomenclature below.

In reaction (3.1) we denote the final-state particles as follows. The Λ, with mass m, is particle 1, and the two tachyons, each of which has liberty mass μ, are denoted as particles 2 and 3. The incident K^- beam momentum is p, and the laboratory energy is denoted by

$$E_l = m_p + (p^2 + m_K{}^2)^{1/2}.$$

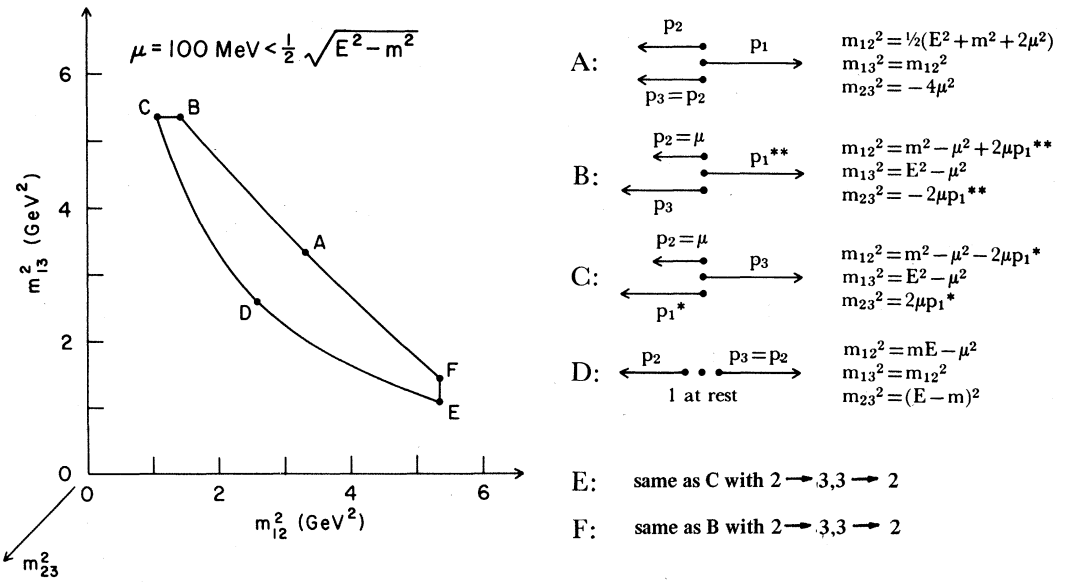

FIG. 1. c.m.-frame Dalitz plot boundary for a Λ (particle 1) recoiling against a pair of tachyons (particles 2 and 3), each having liberty mass $\mu = 100$ MeV, for c.m. energy $E = 2.3$ GeV. The boundary segments *BC* and *EF* are straight lines. Also given are the momentum-vector configurations and invariant mass-squared values at the indicated limiting points along the Dalitz-plot boundary. (The momentum-vector lengths are not drawn to scale.) All quantities in the figure are defined in the text.

The c.m.-frame energy is

$$E=(E_1^2-p^2)^{1/2}.$$

A. c.m.-Frame Dalitz Plot

It is necessary to distinguish two cases which give two distinct Dalitz plots. If

$$2\mu>(E^2-m^2)^{1/2}, \tag{3.4}$$

then it is possible for both tachyons to be simultaneously at liberty, with the Λ taking *all* the energy; this gives the minimum invariant mass squared of the two tachyons as

$$(m_{23}^2)_{\min}^{\text{c.m.}}=-E^2+m^2. \tag{3.5}$$

If, however,

$$2\mu<(E^2-m^2)^{1/2}, \tag{3.6}$$

the minimum c.m.-frame value of m_{23}^2 is greater than the value (3.5). In both cases the maximum value of m_{23}^2 is given by

$$(m_{23}^2)_{\max}=(E-m)^2, \tag{3.7}$$

which corresponds to the Λ being stationary in the c.m. frame; this is also the upper limit when all three final-state particles are ordinary particles.

Figure 1 shows the c.m.-frame Dalitz plot for incident 2.2-GeV/c K^-, giving a c.m. energy of $E=2.3$ GeV; μ is 100 MeV in this figure, so that condition (3.6) holds. Also indicated are the configurations of the three final-state momentum vectors and the invariant masses m_{12}^2, m_{13}^2, m_{23}^2 at limiting points along the plot boundary. The Λ momentum at points C and E is

$$p_1^*=\frac{-\mu(E^2+m^2)+[\mu^2(E^2+m^2)^2+(E^2-\mu^2)(E^2-m^2)^2]^{1/2}}{2(E^2-\mu^2)} \tag{3.8}$$

and at points B and F it is

$$p_1^{**}=\frac{\mu(E^2+m^2)+[\mu^2(E^2+m^2)^2+(E^2-\mu^2)(E^2-m^2)^2]^{1/2}}{2(E^2-\mu^2)}. \tag{3.9}$$

Figure 2 shows the corresponding c.m.-frame Dalitz plot for condition (3.4). The Λ momentum p_1^* at points B and D is the same as that for the Dalitz plot of Fig. 1 [see Eq. (3.8)].

In Fig. 3 the c.m. frame t^+t^- phase space (which is the projection of the Dalitz-plot area onto the m_{23}^2 axis at 45° to the m_{12}^2 and m_{13}^2 axes) is given for a few values of tachyon liberty mass μ at the c.m. energy of this experiment. This figure demonstrates clearly the transition from the Dalitz plot of Fig. 1 to that of Fig. 2.

B. Laboratory-Frame Dalitz Plot

It is again necessary to distinguish two ranges for the tachyon liberty mass which give rise to two different Dalitz plots. If

$$2\mu>p_1^{\dagger}+p, \tag{3.10}$$

where

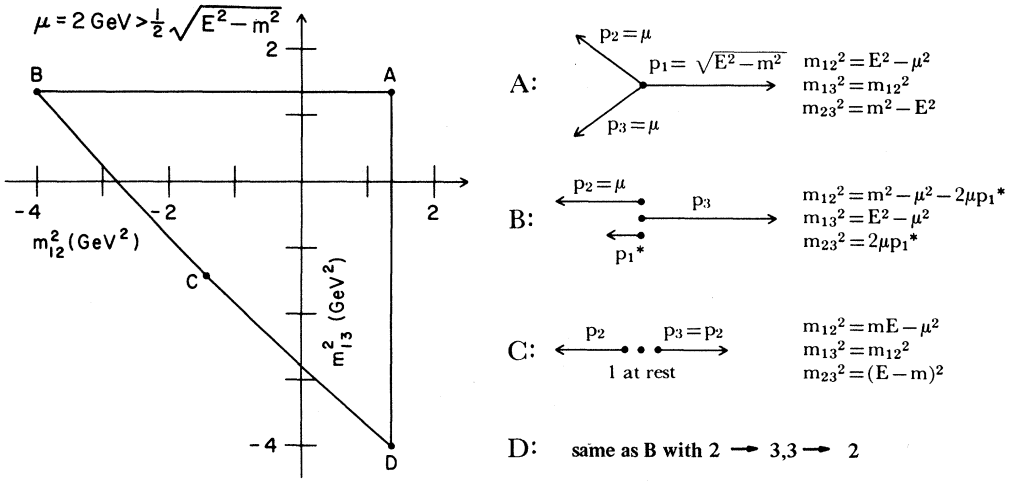

FIG. 2. c.m.-frame Dalitz-plot boundary for a Λ (particle 1) recoiling against a pair of tachyons (particles 2 and 3), each having liberty mass $\mu=2$ GeV, for c.m. energy $E=2.3$ GeV. The boundary segments AB and DA are straight lines. Also given are the momentum-vector configurations and invariant mass-squared values at the indicated limiting points along the Dalitz-plot boundary. (The lengths and angles between the momentum vectors are not drawn to scale.) All quantities in the figure are defined in the text.

$$p_1^{\dagger} \equiv (E_l^2 - m^2)^{1/2}, \tag{3.11}$$

then it is possible for both tachyons to be simultaneously at liberty with the Λ carrying away all the laboratory-frame energy in a direction opposite to that of the beam. In this case the minimum value of t^+t^- invariant mass squared is

$$(m_{23}^2)_{\min}^{\text{lab}} = -(p + p_1^{\dagger})^2, \tag{3.12}$$

which is always smaller than the minimum c.m.-frame value given in Eq. (3.5). When

$$2\mu < p_1^{\dagger} + p, \tag{3.13}$$

the minimum laboratory-frame value of m_{23}^2 is greater than the value (3.12). The maximum value of m_{23}^2 is given by Eq. (3.7), just as in the c.m. frame; this value occurs when the Λ is at rest in the c.m. frame.

Figure 4 is the laboratory-frame Dalitz plot for condition (3.13); also shown is the orientation of the three final-state particle momentum vectors with respect to the incident beam momentum direction at limiting points along the Dalitz-plot boundary. Figure 5 is analogous to Fig. 4 for condition (3.10). The Λ momentum values p_1' and p_1'' indicated in these figures are given by

$$p_1' = \frac{-(\mu - p)B + \{(\mu - p)^2B^2 + [E_l^2 - (\mu - p)^2][B^2 - 4E_l^2m^2]\}^{1/2}}{2[E_l^2 - (\mu - p)^2]} \tag{3.14}$$

and

$$p_1'' = \frac{(\mu - p)B + \{(\mu - p)^2B^2 + [E_l^2 - (\mu - p)^2][B^2 - 4E_l^2m^2]\}^{1/2}}{2[E_l^2 - (\mu - p)^2]}, \tag{3.15}$$

where

$$B \equiv E_l^2 + m^2 + \mu^2 - (\mu - p)^2 = E^2 + m^2 + 2\mu p.$$

In Fig. 6(a) the projection of the laboratory-frame Dalitz plot area onto the m_{23}^2 axis is shown for $\mu = 1$, 2, and 5 GeV, showing how the area of the Dalitz plot grows with μ. The phase space is not proportional to the area of the Dalitz plot in the laboratory frame, however. The laboratory-frame Lorentz-invariant[27] phase space is given by

$$\rho = \int \left(\frac{p_2}{p \sin\varphi_{23}} \right) dE_2\, dE_3 d\theta_{2p} d\theta_{23}. \tag{3.16}$$

All the variables in this expression are given in the laboratory frame. p_2 is the three-momentum of particle 2; E_2 and E_3 are the energies of particles 2 and 3. θ_{2p} is the angle between the momentum vectors of particle 2 and the beam; θ_{23} is that between the momentum vectors of particles 2 and 3; and φ_{23} is the azimuth of the momentum vector of particle 3 in a reference frame in which the direction of particle 2 is the z axis and the plane of the three-momenta of particle 2 and the beam define $\varphi = 0$. Figure 6(b) is the laboratory-frame phase space calculated by numerical integration of Eq. (3.16) for tachyon liberty masses of 1, 2, and 5 GeV. The phase space approaches a constant value for $\mu \gtrsim 5$ GeV.

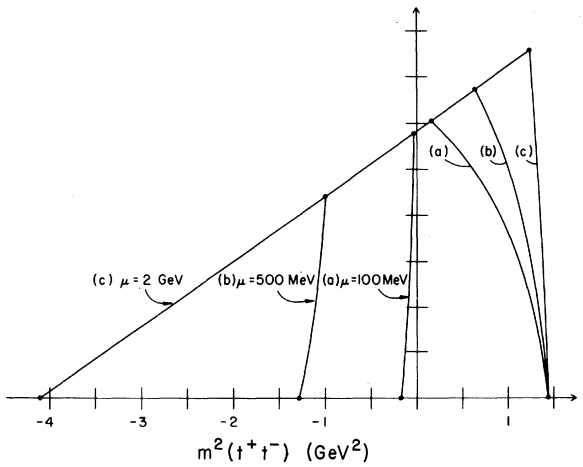

FIG. 3. Phase-space distribution (in arbitrary units) of tachyon-pair (t^+, t^-) invariant mass squared in the c.m. frame for two tachyons and a Λ in the final state at c.m. energy $E = 2.3$ GeV. The phase space, which is the projection of Dalitz-plot area onto the $m^2(t^+t^-)$ axis, is given for three indicated values of tachyon liberty mass μ.

C. Comparison between c.m.-Frame and Laboratory-Frame Dalitz Plots

Note that if the tachyon liberty mass is small enough for condition (3.6) to be satisfied in the c.m. frame, then condition (3.13) will always hold in the laboratory frame. If, however, condition (3.4) is true in the c.m. frame, then either (3.10) or (3.13) can hold in the laboratory frame. Thus the Dalitz plot of Fig. 1 in the c.m. frame always becomes that of Fig. 4 in the laboratory frame, whereas the c.m. Dalitz plot of Fig. 2 can go over into that of Fig. 4 or 5 in the laboratory frame. Conversely, note that laboratory-frame condition

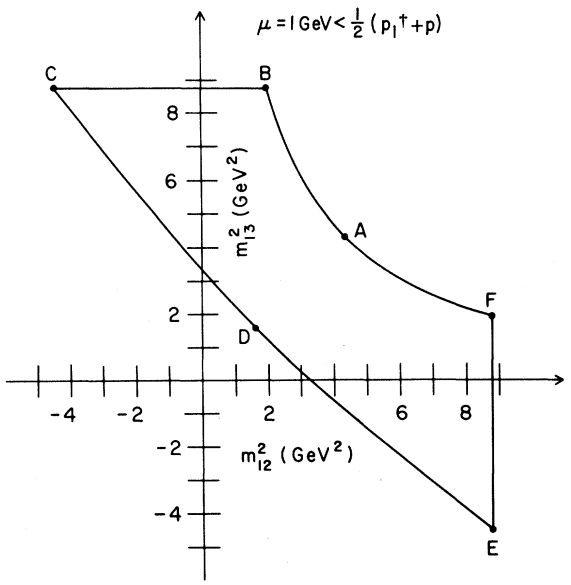

A: p_1, p_2, $p_3 = p_2$, p
$m_{12}^2 = \frac{1}{2}(E^2 + m^2 + 2\mu^2)$
$m_{13}^2 = m_{12}^2$
$m_{23}^2 = -4\mu^2$

B: p_1'', $p_2 = \mu$, p_3, p
$m_{12}^2 = m^2 - \mu^2 + 2\mu p_1''$
$m_{13}^2 = E^2 - \mu^2 + 2\mu p$
$m_{23}^2 = -2\mu(p + p_1'')$

C: p_3, $p_2 = \mu$, p_1', p
$m_{12}^2 = m^2 - \mu^2 - 2\mu p_1'$
$m_{13}^2 = E^2 - \mu^2 + 2\mu p$
$m_{23}^2 = 2\mu(p_1' - p)$

all configurations with

D: $p_1 = (m/E)p$, p
$m_{12}^2 = mE - \mu^2$
$m_{13}^2 = m_{12}^2$
$m_{23}^2 = (E - m)^2$

E: same as C with 2 → 3,3 → 2

F: same as B with 2 → 3,3 → 2

FIG. 4. Laboratory-frame Dalitz-plot boundary for a Λ (particle 1) recoiling against a pair of tachyons (particles 2 and 3), each having liberty mass $\mu = 1$ GeV, for beam momentum $p = 2.2$ GeV/c (laboratory-frame energy $E_l = 3.1$ GeV). The boundary segments BC and EF are straight lines. Also given are the momentum-vector configurations for all three final-state particles with respect to the beam momentum vector p, and invariant mass-squared values at the indicated limiting points along the Dalitz-plot boundary. (The momentum-vector lengths are not drawn to scale.) We note that at B and F the direction of p_1'' is reversed if $\mu < \frac{1}{2}p - (E_l - m)^2/2p$; at A the direction of p_1 is reversed if $\mu^2 < (\frac{1}{2}p)^2 - [\frac{1}{2}(E_l - m)]^2$. All quantities in the figure are defined in the text.

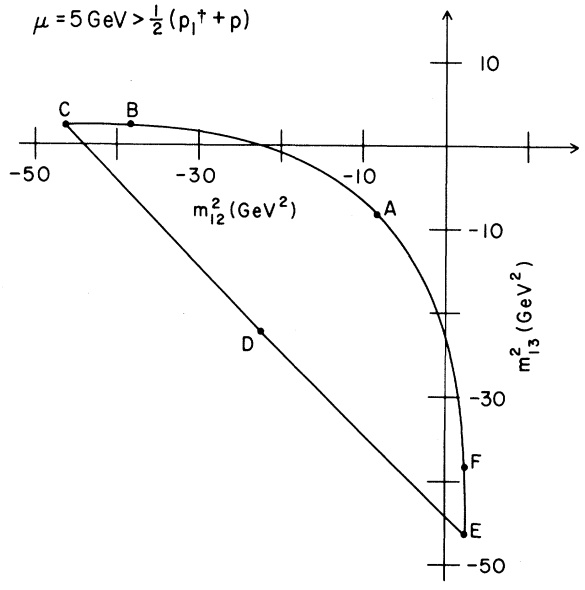

A: $p_1^\dagger$, $p_2 = \mu$, $p_3 = \mu$, p
$m_{12}^2 = E^2 + p^2 - \mu^2 + pp_1^\dagger$
$m_{13}^2 = m_{12}^2$
$m_{23}^2 = -(p + p_1^\dagger)^2$

B: $p_3 = \mu$, $p_2 = \mu$, p, $p_1^\dagger$
$m_{12}^2 = m^2 - \mu^2 - 2\mu p + \mu(E^2 - m^2)/(\mu - p)$
$m_{13}^2 = E^2 - \mu^2 + 2\mu p$
$m_{23}^2 = -\mu(E^2 - m^2)/(\mu - p)$

C: p_3, $p_2 = \mu$, p, p_1'
$m_{12}^2 = m^2 - \mu^2 - 2\mu p_1'$
$m_{13}^2 = E^2 - \mu^2 + 2\mu p$
$m_{23}^2 = 2\mu(p_1' - p)$

all configurations with

D: $p_1 = (m/E)p$, p
$m_{12}^2 = mE - \mu^2$
$m_{13}^2 = m_{12}^2$
$m_{23}^2 = (E - m)^2$

E: same as C with 2 → 3,3 → 2

F: same as B with 2 → 3,3 → 2

FIG. 5. Laboratory-frame Dalitz-plot boundary for a Λ (particle 1) recoiling against a pair of tachyons (particles 2 and 3), each having liberty mass $\mu = 5$ GeV, for beam momentum $p = 2.2$ GeV/c (laboratory-frame energy $E_l = 3.1$ GeV). The boundary segments BC and EF are straight lines. Also given are the momentum-vector configurations for all three final-state particles with respect to the beam momentum vector p, and invariant mass-squared values at the indicated limiting points along the Dalitz-plot boundary. (The lengths and angles between the momentum vectors are not drawn to scale.) We note that at B and F the angle between p_2 and p_3 is less than $\frac{1}{2}\pi$ if $\mu^2 + (\mu - p)^2 < p_1^{\dagger 2}$. All quantities in the figure are defined in the text.

(3.10) implies condition (3.4) in the c.m. frame, whereas if condition (3.13) holds, then either (3.4) or (3.6) can be true in the laboratory frame. The relationship between the c.m.-frame and laboratory-frame Dalitz plots is illustrated in Fig. 7 for the energy used in this experiment.

IV. ANALYSIS OF DATA

The events studied in this search appear as a beam-track (2.2-GeV/c K^-) interaction with a target proton producing two outgoing charged tracks and an associated positively identified Λ decaying into a proton and a π^-. To facilitate the identification of the neutral decay particle as a Λ, the scanning criteria allow the selection of low-energy

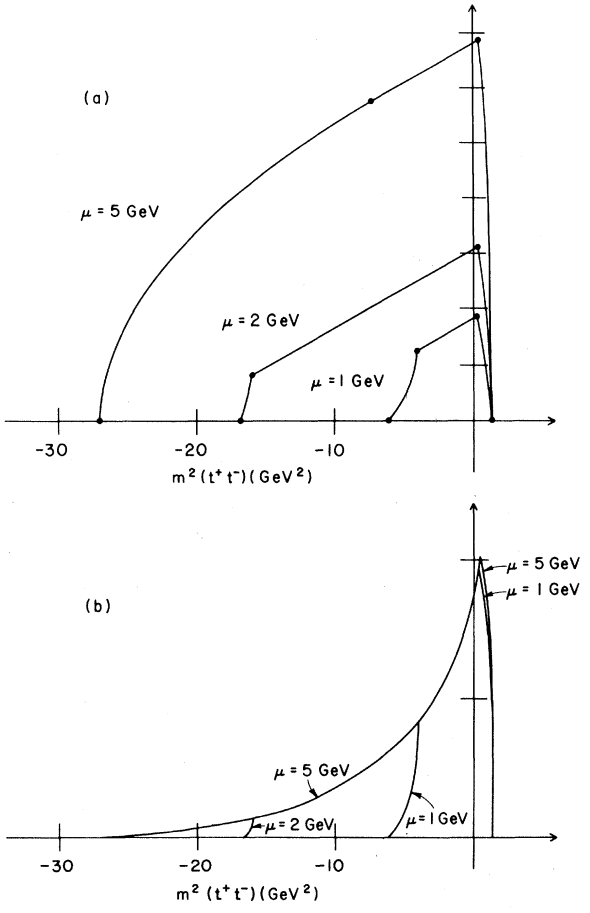

FIG. 6. Laboratory-frame variables for the case of a Λ recoiling against a pair of tachyons for K^- beam momentum p = 2.2 GeV/c (laboratory-frame energy E_l = 3.1 GeV). Results are shown for three indicated values of tachyon liberty mass μ. (a) Projection of the laboratory-frame Dalitz-plot area (in arbitrary units) onto the tachyon-pair (t^+,t^-) invariant-mass-squared axis. (b) Phase-space distribution (in arbitrary units) of tachyon-pair invariant-mass squared in the laboratory frame.

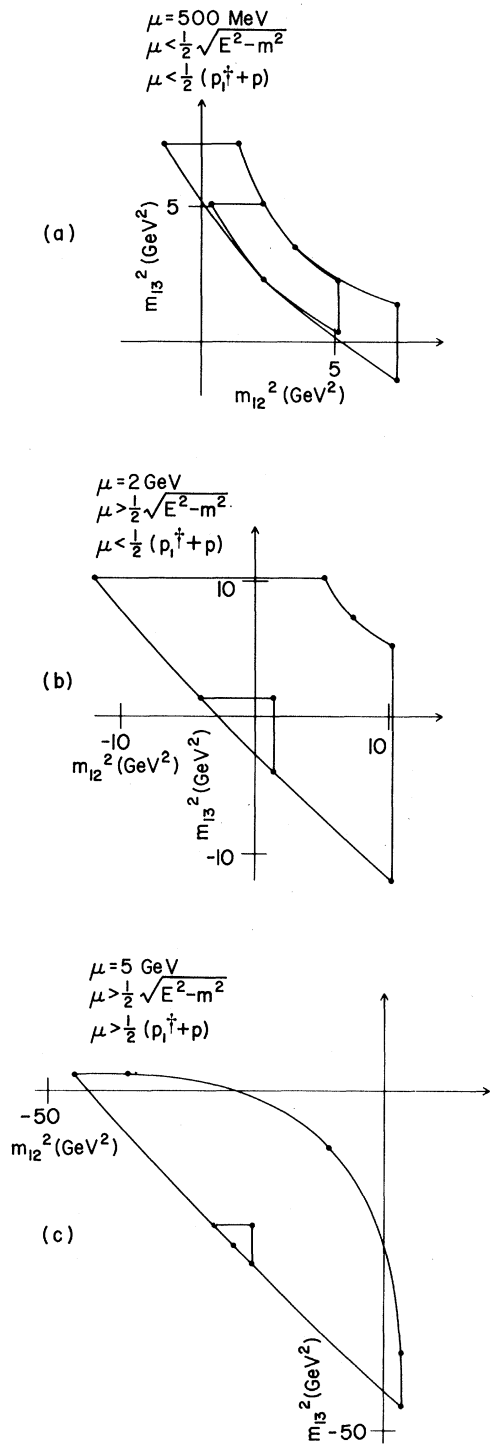

FIG. 7. Comparison between c.m.-frame and laboratory-frame Dalitz plots for a Λ (particle 1) and two tachyons (particles 2 and 3) of liberty mass μ in the final state. The K^- beam momentum is p = 2.2 GeV/c, laboratory-frame energy is E_l = 3.1 GeV, c.m.-frame energy is E = 2.3 GeV. In all cases the inner Dalitz-plot boundary is that for the c.m. frame. (a) μ = 500 MeV, (b) μ = 2 GeV, (c) μ = 5 GeV.

($E_\Lambda \lesssim 1.55$ GeV) Λ's only, the positive decay track of which can be readily identified as a proton. This procedure yields a sample of Λ's produced with four-momentum transfer squared t from the proton of less than about 0.8 GeV^2 in magnitude.

The production reaction hypotheses are

$K^-p \to \Lambda\pi^+\pi^-$

$\to \Lambda\pi^+\pi^-\gamma$

$\to \Lambda\pi^+\pi^-\pi^0$

$\to \Lambda\pi^+\pi^-\eta$

$\to \Lambda\pi^+\pi^-$ + more than 1 unseen neutral

$\to \Lambda K^+K^-$

$\to \Lambda K^+K^-\gamma$

$\to \Lambda K^+K^-\pi^0$

$\to \Lambda K^+K^-$ + more than 1 unseen neutral

$\to \Sigma^0 K^+K^-$, $\Sigma^0 \to \Lambda\gamma$

$\to \Sigma^0\pi^+\pi^-$, $\Sigma^0 \to \Lambda\gamma$

$\to \Lambda K^+\pi^-\bar{K}^0$ (unseen $\bar{K}^0$ decay)

$\to \Lambda K^-\pi^+K^0$ (unseen K^0 decay)

$\to \Lambda K^\pm\pi^\mp$ + unseen kaon and ≥ 1 unseen neutral

$\to \Xi^0 K^+\pi^-$, $\Xi^0 \to \Lambda\pi^0$.

In these hypotheses, "unseen neutral" means γ, π^0, or η. We do not try fits to reactions having a Ne nucleus as target, despite an admixture of four molar percent Ne in the bubble chamber; most Ne interactions are rejected during scanning.

Every event of the type (2.1) can be interpreted as the final state $\Lambda\pi^+\pi^-$(MM), where (MM) denotes the missing four-momentum necessary to balance the measured initial- and final-state momentum and energy of the visible tracks. As was explained in Sec. II, examples of the reaction $K^-p \to \Lambda t^+t^-$ should have a negative missing energy (within errors) when the final state is interpreted as $\Lambda\pi^+\pi^-$(MM). We therefore restrict our attention only to those events for which the missing energy in the interpretation $\Lambda\pi^+\pi^-$(MM) is less than zero. We will, however, reject any event having a successful interpretation as any of the above reaction hypotheses with one or no missing neutrals. A "successful" interpretation is one with a confidence level for the fit of greater than 0.1%. We shall return later to an estimate of how the neglect of events fitting any of the above-mentioned hypotheses affects the range of tachyon masses to which we are sensitive.

A sample of about 1900 events [of 21 000 events of the topology (2.1)] having negative missing energy for the final-state interpretation $\Lambda\pi^+\pi^-$(MM) was considered. Already excluded from this sample are all events fitting the final state $\Lambda\pi^+\pi^-\gamma$, for reasons particular to our fitting procedure.

Most of the selected events with negative missing energy are examples of the reaction $K^-p \to \Lambda\pi^+\pi^-$ for which uncertainty in the beam momentum determination caused the missing energy to be negative when the track measurements are used in the interpretation $\Lambda\pi^+\pi^-$(MM); in most of these cases the magnitude of the missing energy is less than 100 MeV. Figure 8 is a scatter plot of missing energy vs the component of missing momentum parallel to the beam direction; the figure contains most of the $\approx$1900 events considered. The heavy diagonal band in this figure is defined by events for which the (negative) missing energy is nearly equal to the component of missing momentum parallel to the beam direction. About 1500 of the approximately 1650 events comprising the prominent diagonal band of Fig. 8 have a fit to the final state $\Lambda\pi^+\pi^-$. The remaining $\approx$150 events in this band which do *not* fit $\Lambda\pi^+\pi^-$ were found nevertheless to be mostly examples of this final state, as was evidenced by a comparison of the $\pi^+\pi^-$ invariant mass spectrum for these events with that of events having a successful fit to $\Lambda\pi^+\pi^-$. This sample of events presumably does not fit the final state $\Lambda\pi^+\pi^-$ because of a somewhat incorrect assignment of beam momentum or beam momentum error to these events in the beam momentum averaging procedure. Since almost all events in the diagonal band of Fig. 8 are examples of the final state

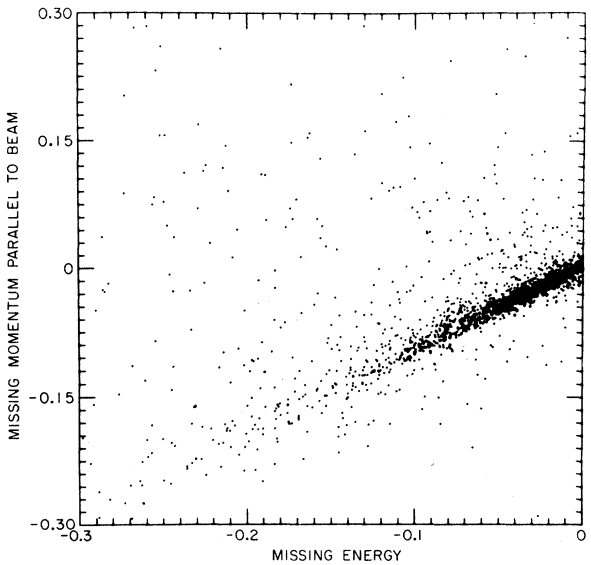

FIG. 8. Missing energy (in GeV) vs component of missing momentum parallel to the beam direction (in GeV/c) for events with negative missing energy for the final-state interpretation $\Lambda\pi^+\pi^-$(MM). The plot does not contain events fitting the final state $\Lambda\pi^+\pi^-\gamma$ (see text).

$\Lambda\pi^+\pi^-$, we exclude them from consideration. We do this by ignoring events for which the missing energy is equal within ±50 MeV to the component of missing momentum parallel to the beam direction. After this cut, ≈250 events remain.

One further cut was imposed to reduce the background in the sample of events most likely to be true examples of tachyon pair production. Events for which the absolute value of the missing momentum was greater than the magnitude of the missing energy were excluded. As stated above, the opposite condition is expected to hold if tachyon pairs are produced (yielding zero missing momentum and negative missing energy) – that is to say, the missing mass squared is expected to be positive for the final state Λt^+t^- interpreted as $\Lambda\pi^+\pi^-$(MM). However, it is well known that events from the four-constraint (at the production vertex) final state $\Lambda\pi^+\pi^-$ with one mismeasured track will, if interpreted as $\Lambda\pi^+\pi^-$(MM), have a missing momentum larger in magnitude than the missing energy (i.e., negative missing mass squared). Furthermore, the missing energy for a sample of mismeasured four-constraint events is just as likely to be positive as negative; this fact allows a check of the events excluded by demanding positive missing mass squared for the interpretation $\Lambda\pi^+\pi^-$(MM). A plot (not shown) of missing energy vs magnitude of missing momentum for all events interpreted as $\Lambda\pi^+\pi^-$(MM) shows that of the events with $|\vec{p}(\mathrm{MM})|$ (missing momentum) greater than $|E(\mathrm{MM})|$ (missing energy), there are as many events with $E(\mathrm{MM})>0$ as with $E(\mathrm{MM})<0$, and the distribution of $|\vec{p}(\mathrm{MM})|$ versus $E(\mathrm{MM})$ for $E(\mathrm{MM})<0$ is the same as that for $E(\mathrm{MM})>0$. About 60 additional events are excluded by requiring $|E(\mathrm{MM})|>|\vec{p}(\mathrm{MM})|$.

We will consider below the bias against true examples of tachyon production introduced by the two cuts described above. After applying these cuts to all events having negative missing energy in the interpretation $\Lambda\pi^+\pi^-$(MM), there remain 179 events. Each of these events was carefully examined on the scan table.

Using the track measurement information for each event, all but about 50 of these events were immediately removed from consideration, for one of the following reasons:

(1) The event had been grossly misidentified (e.g., the primary interaction vertex exhibited short proton or nuclear fragment tracks indicating an interaction with a nucleus of Ne; a stray track had been incorrectly identified as a Λ decay).

(2) The measured momentum of a track in the event was greatly in error.

(3) The event had a successful overdetermined fit to one or more of the reaction hypotheses listed at the beginning of this section.

(4) Some events which had been measured more than once had, from another measurement, a successful overdetermined fit to one or more of the reaction hypotheses given at the beginning of this section.

(5) The bubble density of one or more of the tracks in the event led to an unambiguous determination that the particle claimed to be a Λ decay was in fact a $\overline{K}^0$ decay or an e^+e^- pair, or that a track from the primary vertex was a $K^\pm$ or proton.

For the remaining events it was impossible to conclusively identify tracks on the basis of bubble density. These events were processed with an expanded kinematic fitting program which allowed, in addition to the reaction hypotheses given at the beginning of this section, additional hypotheses in which the neutral decay was fitted as $\overline{K}^0\to\pi^+\pi^-$. All but 11 of the events thus processed were then rejected, in most cases because the event had a good fit to the final state $\overline{K}^0p\pi^-$ or $\overline{K}^0p\pi^-\pi^0$. In all such cases the visual bubble density estimates for the tracks in the event were consistent with the results of the fit. In several cases an event was rejected because the detailed measurement and fit information revealed that the event had been misidentified (e.g., a stray track was measured as a primary interaction track) or mismeasured (e.g., a small-angle scatter on a track had not been noticed and had been ignored in the measurement).

It had been noted in the examination of many of the rejected events that some events had both a positively identified proton and a positively identified Λ in the final state – these events were rejected because they could be plausibly explained as a K^- interaction with both a neutron and a proton in a Ne nucleus; i.e., as $K^-pn\to\Lambda p\pi^-$ + possible unseen neutrals.[28] For the remaining 11 events a Λ was the most likely interpretation of the decay interaction, and in most cases the positive track from the primary interaction had minimum bubble density with a momentum too high ($p\gtrsim 1.5$ GeV/c) to allow the track to be identified. These 11 events were fitted as K^-d interactions (approximating the suspected interaction of the K^- with a proton and a neutron in a Ne nucleus by an interaction with a stationary deuteron). All but one of these events were found to be interpretable as the reactions $K^-d\to\Lambda p\pi^-$, $\Sigma^0p\pi^-$, $\Lambda p\pi^-\pi^0$, $\Lambda n\pi^+\pi^-$, or $\Lambda\Sigma^-K^+$. In all cases the results of the fits were in agreement with the observed track bubble densities.

The one event which did not fit an hypothesis as a K^-d interaction, when interpreted as $K^-d\to\Lambda p\pi^-$, conserved energy to within 15 MeV. However, the momentum imbalance for this event, 350 ± 50 MeV/c, prevented a fit as a K^-d interaction. This circumstance is consistent with the interpretation

that the K^- beam interacted with two nucleons (i.e., a deuteron) in a Ne nucleus, and that this target had a Fermi momentum of ≈ 350 MeV/c at the time of interaction. This momentum would imply only a very small target energy uncertainty (of order 10–20 MeV); a heavy nuclear fragment recoiling against the two target nucleons could then be invisible. In any case, as stated above, we expect candidates for tachyon pair production to exhibit no momentum imbalance, within measurement errors. We conclude that this event has a more likely explanation as the result of a K^- interaction with a nucleus of Ne. (We note that Ne interactions are not rare; the admixture of Ne in the bubble chamber is such that there is one Ne interaction for every ten beam interactions with a proton.)

We thus find that all 179 events examined as possible examples of tachyon pair production via $K^-p \to \Lambda t^+ t^-$ can be explained as ordinary interactions. Furthermore, none of the examined events had primary interaction tracks with bubble density obviously less than that of minimum-ionizing beam tracks. Many of the examined events would have had one or both primary interaction tracks with indentifiably less than minimum bubble density if these tracks had been made by tachyons, assuming a bubble density proportional to $1/\beta^2$. The expected tachyon bubble density was obtained by calculating, if possible, the tachyon liberty mass required to produce energy balance for each examined event. In particular, it does not seem likely that the 11 events interpreted as K^-d interactions are examples of $K^-p \to \Lambda t^+ t^-$. Five of these events do not have missing momentum consistent with zero in the interpretation $\Lambda\pi^+\pi^-$(MM). The tachyon liberty masses calculated for these events do not cluster near any particular value, and all 11 events would have at least one tachyon track with bubble density (assumed $\sim 1/\beta^2$) less than 70% that of minimum-ionizing beam tracks.

The fact that every examined event can be plausibly accounted for as an ordinary interaction does not of course exclude the possibility that some of them might be examples of tachyon pair production. However, since we have no clear candidate for the reaction $K^-p \to \Lambda t^+ t^-$, we prefer to interpret our results as a lack of conclusive evidence for the production of ionizing tachyons. We claim as a safe upper limit that there are fewer than four interactions of the type searched for, giving a cross-section upper limit of ≈ 0.2 μb.

In order to state the range of tachyon liberty masses and of tachyon-pair invariant masses for which we have found a cross section upper bound (under our assumptions), we examine the limits imposed by the following:

(a) The assumption, stated in Sec. II, that we do not expect to detect ionizing tachyons if their velocity is much greater than $v \cong 1.7c$ (i.e., we require $1/\beta^2 \gtrsim \frac{1}{3}$).

(b) The fact that the scanning criteria in this experiment restrict the accepted Λ's to have laboratory energies of $\lesssim 1.55$ GeV (giving a momentum-transfer-squared upper limit of $|t| \lesssim 0.8$ GeV^2) and to recoil at an angle not greater than 90° with respect to the beam.

(c) The cuts imposed to reduce the background in the sample of events most likely to be examples of charged tachyon pair production.

(d) The possible loss of true examples of tachyon pair production caused by neglecting events having a successful constrained fit to any of the reaction hypotheses given at the beginning of this section.

We will show that condition (a) implies an upper limit on the liberty masses of the tachyons that we would be able to detect; that condition (b) gives a lower limit on the tachyon-pair invariant masses that we can examine, as well as a limit on the momentum transfer range considered; and that cuts (c) and consideration (d) yield an approximate lower limit for the tachyon liberty masses. We consider each condition in turn.

First, the restriction that both tachyons have laboratory-frame velocities less than some value gives an upper limit for the liberty mass of each tachyon. This is true because the available laboratory-frame energy is fixed, and as the liberty mass of each tachyon (and thus the minimum tachyon momentum) is increased, a liberty mass will be reached for which the ratio p/E (= tachyon velocity) must always be greater than the predetermined value. In order to find the tachyon liberty-mass upper limit implied by our choice of $\beta_{\text{tachyon}} < 1.7$ for each tachyon, the laboratory-frame phase space for tachyon pair production via reaction (2.2) was generated with this restriction imposed, as well as with the two restrictions on the recoil Λ stated in (b) above. The condition that the velocity of each tachyon be less than $1.7c$ yields an upper limit of ≈ 1 GeV for the tachyon liberty mass.

The conditions on the recoil Λ stated in (b) imply an efficiency for detecting tachyon pairs with negative invariant mass squared which is sharply reduced in comparison to pairs with positive invariant mass squared. This affects pairs with large liberty mass more than those with small liberty mass, since the allowed lower limit of tachyon-pair invariant mass squared becomes smaller as the liberty mass μ grows from 0 to about 5 GeV (see Fig. 6). In fact, for $\mu \lesssim 200$ MeV, only a small fraction of the phase space extends to negative values of tachyon-pair mass squared. The

combined effects of the conditions on the recoil Λ and the changing kinematic lower limit of tachyon-pair invariant mass squared give roughly constant phase space for $0 \lesssim \mu \lesssim 1$ GeV and for $0 < m^2(t^+t^-) < 1.44$ GeV^2 (1.44 GeV^2 is the maximum allowed tachyon-pair invariant mass squared at our energy), although we are somewhat sensitive to negative $m^2(t^+t^-)$ out to about -1 GeV^2 for $\mu = 500$ MeV and out to about -2 GeV^2 for $\mu = 1$ GeV. For simplicity, however, we prefer to quote a cross-section bound for positive $m^2(t^+t^-)$ only, for which the phase space in our experiment is roughly constant for $\mu \lesssim 1$ GeV. We base our sensitivity only upon the amount of phase space available for each value of μ, ignoring the possible effect of an unknown matrix element.

Now we consider the effects of the above-described cuts made to eliminate mismeasured events and events which are actually examples of the final state $\Lambda\pi^+\pi^-$, and the effect of measurement uncertainties. These considerations affect the detection of pairs of tachyons with small liberty masses. If there were no measurement uncertainties, the negative missing energy E(MM) obtained as a consequence of interpreting the final state Λt^+t^- as $\Lambda\pi^+\pi^-$(MM) would be

$$|E(\mathrm{MM})| = (p_+^2 + m_\pi^2)^{1/2} + (p_-^2 + m_\pi^2)^{1/2} - (p_+^2 - \mu^2)^{1/2} - (p_-^2 - \mu^2)^{1/2}.$$

Here p_+ and p_- are the laboratory momenta of the two outgoing charged tracks. Now p_+ and p_- are seldom smaller than 500 MeV/c, and are typically 1 GeV/c in this experiment. Thus $m_\pi^2 \ll p_+^2, p_-^2$ is almost always a good approximation, and if we consider $\mu \lesssim 500$ MeV (from the above, we only consider $\mu < 1$ GeV anyway), we also have $\mu^2 \ll p_+^2$, p_-^2. For these limits, we get

$$|E(\mathrm{MM})| \cong \frac{m_\pi^2 + \mu^2}{2}\left(\frac{1}{p_+} + \frac{1}{p_-}\right).$$

If we take $p_+ \approx p_- \approx 1$ GeV/c, we have

$$|E(\mathrm{MM})| \cong f(m_\pi^2 + \mu^2), \quad f \approx 1. \tag{4.1}$$

This shows how μ is correlated with increasing values of missing energy for small values of μ. There are, however, other errors which sometimes yield negative missing energy even when the mass of the outgoing primary interaction tracks is correctly assigned. The main source of this error is the uncertainty in the beam momentum; as was discussed above, most of the events having negative missing energy when interpreted as $\Lambda\pi^+\pi^-$(MM) (see Fig. 8) are examples of the final state $\Lambda\pi^+\pi^-$ for which the magnitude of the missing energy is equal (within less than ±50 MeV) to the component of missing momentum parallel to the beam direction. The uncertainty in the beam momentum yields a missing energy given by

$$E(\mathrm{MM}) \cong p_{\mathrm{par}}(\mathrm{MM}), \tag{4.2}$$

where p_{par}(MM) is the component of missing momentum parallel to the beam direction. Equations (4.1) and (4.2) describe independent sources of the missing energy for the interpretation $\Lambda\pi^+\pi^-$(MM); the first depends on the mass assignment and the momentum of the outgoing primary tracks, and the second depends on the beam momentum determination. The over-all missing energy in the interpretation of events as $\Lambda\pi^+\pi^-$(MM) should then simply be the sum of the right-hand sides of Eqs. (4.1) and (4.2). To verify this simple behavior, we have recalculated the missing energy for events from the final state $\Lambda\pi^+\pi^-$ using as the pion mass 300 MeV instead of the correct value of 140 MeV. It was then seen that the new missing energy was contained in a band of the E(MM) vs p_{par}(MM) plot more negative in E(MM) by about 100 MeV. From a calculation analogous to that leading to expression (4.1), this result implies $f \cong 1.4$ in Eq. (4.1).

We thus expect any appreciable amount of tachyon pair production with a fixed tachyon liberty mass to appear as a diagonal band in Fig. 8 parallel to and to the left of the band defined by the $\Lambda\pi^+\pi^-$ events. Since we exclude from consideration any event for which the missing energy is equal within ±50 MeV to the component of missing momentum parallel to the beam direction, we expect to be less sensitive to tachyon pairs whose liberty masses are smaller than the value which would give a missing energy of about -50 MeV from Eq. (4.1). Using a conservative value of $f = 1.2$ in this equation, we conclude that we are less sensitive to tachyon liberty masses smaller than about 140 MeV. The fact that we consider only negative values of E(MM) with $|E(\mathrm{MM})| > |\vec{p}(\mathrm{MM})|$ similarly yields a reduced detection efficiency for tachyon liberty masses below about 150 MeV. For simplicity, we summarize the combined effects of the experimental cuts and the measurement uncertainties by quoting $\mu = 100$ MeV as the lowest value of liberty mass we can reliably detect.

Finally we consider the effect of ignoring as a candidate for tachyon pair production any event having a successful fit to one or more of the overdetermined reaction hypotheses given at the beginning of this section. In the preceding paragraph we have already noted the effect of the cut made to exclude events which fit the final-state hypothesis $\Lambda\pi^+\pi^-$ and which have negative missing energy when interpreted as $\Lambda\pi^+\pi^-$(MM). The only other final states containing appreciable numbers of events with negative missing energy in the in-

terpretation $\Lambda\pi^+\pi^-$(MM) are $\Lambda\pi^+\pi^-+1$ missing neutral [about 70 events with negative E(MM)] and $\Sigma^0\pi^+\pi^-$ [about 260 events with negative E(MM)]. An examination of these events shows that all but about 10% of them would lie in the same band of Fig. 8 [$E(\mathrm{MM}) = p_{\mathrm{par}}(\mathrm{MM}) \pm 50$ MeV] as most examples of the final state $\Lambda\pi^+\pi^-$ with negative E(MM). Thus the exclusion from consideration as tachyon production of events having a successful constrained fit does not alter our estimate obtained in the preceding paragraph for the range of tachyon liberty masses that we expect to be able to detect.

V. CONCLUSION

We have examined the possibility that visible ionization tracks in reaction (2.1) observed in a bubble chamber could be examples of tachyon pair production via the reaction $K^-p \to \Lambda t^+ t^-$. The assumptions we have made about tachyons for this search are discussed in Sec. II, where they are compared with the assumptions made in other tachyon searches. The fact that we find fewer than four events for an exposure size of 20 events/μb implies a cross section upper limit, under our assumptions, of ≈ 0.2 μb for pairs of tachyons having liberty masses between ≈ 100 MeV and ≈ 1 GeV, for pair invariant mass-squared values between 0 and 1.44 GeV^2, and for proton-to-Λ momentum transfer squared between 0 and about -0.8 GeV^2.

ACKNOWLEDGMENTS

We gratefully acknowledge helpful discussions with Professor G. Feinberg. The film for this experiment was scanned and measured in the Bubble Chamber Group at BNL and at the University of Michigan; the data analysis was performed with the assistance of the staff of the BNL Central Scientific Computing Facility. We thank Dr. R. P. Shutt and Dr. N. P. Samios for their support and encouragement.

---

*Work supported by the U. S. Atomic Energy Commission.

†Permanent address: York College, City University of New York, Queens, N.Y.

[1]O. M. P. Bilaniuk, V. K. Deshpande, and E. C. G. Sudarshan, Am. J. Phys. 30, 718 (1962). See also H. Schmidt, Z. Physik 151, 365 (1958); 151, 408 (1958); S. Tanaka, Progr. Theoret. Phys. (Kyoto) 24, 171 (1960); Ya. P. Terletskii, Dokl. Akad. Nauk SSSR 133, 329 (1960) [Soviet Phys. Doklady 5, 782 (1960)].

[2]G. Feinberg, Phys. Rev. 159, 1089 (1967).

[3]M. E. Arons and E. C. G. Sudarshan, Phys. Rev. 173, 1622 (1968).

[4]J. Dhar and E. C. G. Sudarshan, Phys. Rev. 174, 1808 (1968); David G. Boulware, Phys. Rev. D 1, 2426 (1970); E. C. G. Sudarshan, *ibid.* 1, 2428 (1970).

[5]K. H. Mariwalla, Am. J. Phys. 37, 1281 (1969); V. S. Olkhovsky and E. Recami, Lett. Nuovo Cimento 1, 165 (1971).

[6]A. Peres, Lett. Nuovo Cimento 1, 837 (1969).

[7]F. Salzman and G. Salzman, Lett. Nuovo Cimento 1, 859 (1969).

[8]M. Glück, Nuovo Cimento 62A, 791 (1969).

[9]V. S. Olkhovsky and E. Recami, Nuovo Cimento 63A, 814 (1969).

[10]M. Baldo and E. Recami, Lett. Nuovo Cimento 2, 643 (1969).

[11]M. Baldo, G. Fonte, and E. Recami, Lett. Nuovo Cimento 4, 241 (1970).

[12]M. Glück, Nuovo Cimento 67A, 658 (1970).

[13]Robert G. Cawley, Phys. Rev. D 2, 276 (1970).

[14]A. M. Gleeson, M. G. Gundzik, E. C. G. Sudarshan, and Antonio Pagnamenta, Particles and Nuclei 1, 1 (1970).

[15]Roger G. Newton, Phys. Rev. 162, 1274 (1967); Science 167, 1569 (1970).

[16]William B. Rolnick, Phys. Rev. 183, 1105 (1969).

[17]O.-M. Bilaniuk and E. C. G. Sudarshan, Nature 223, 386 (1969).

[18]R. Fox, C. G. Kuper, and S. G. Lipson, Nature 223, 597 (1969); Proc. Roy. Soc. (London) A316, 515 (1970).

[19]D. J. Thouless, Nature 224, 506 (1969).

[20]Paul L. Csonka, Nucl. Phys. B21, 436 (1970).

[21]F. A. E. Pirani, Phys. Rev. D 1, 3224 (1970).

[22]E. Recami, Lett. Nuovo Cimento 4, 73 (1970).

[23]G. A. Benford, D. L. Book, and W. A. Newcomb, Phys. Rev. D 2, 263 (1970).

[24]O.-M. Bilaniuk and E. C. G. Sudarshan, Phys. Today 22 (No. 5), 43 (1969); O.-M. Bilaniuk *et al.*, *ibid.* 22 (No. 12), 47 (1969); 23 (No. 5), 13 (1970); 24 (No. 3), 14 (1971).

[25]Torsten Alväger and Michael N. Kreisler, Phys. Rev. 171, 1357 (1968); M. B. Davis, M. N. Kreisler, and T. Alväger, *ibid.* 183, 1132 (1969).

[26]C. Baltay, G. Feinberg, N. Yeh, and R. Linsker, Phys. Rev. D 1, 759 (1970).

[27]The laboratory-frame phase space is Lorentz invariant in the sense that it is defined as

$$\rho = \int \frac{d^3p_1}{2E_1}\frac{d^3p_2}{2E_2}\frac{d^3p_3}{2E_3}\,\delta^4(p_{\mathrm{total}} - p_1 - p_2 - p_3)\,.$$

However, a Lorentz transformation to another frame can change the phase space, because, for instance, some allowed three-particle configurations in the laboratory frame can transform into configurations in which one or both tachyons have negative energy. Such configurations involving negative tachyon energies are then reinterpreted as examples of a different reaction and thus lost from the phase space of the original reaction [see the discussion of reactions (3.1)–(3.3)].

[28]We note that K^- interactions with two nucleons are commonly observed in K^- He interactions; see, for instance, P. O. Mazur *et al.*, Phys. Rev. D 1, 20 (1970).